ACS APPLIED MATERIALS & INTERFACES

Research Article

www.acsami.org

Graphene Oxide Selectively Enhances Thermostability of Trypsin

Kai Yao, Pengli Tan, Yinchan Luo, Liangzhu Feng, Ligeng Xu, Zhuang Liu, Youyong Li,* and Rui Peng*

Institute of Functional Nano and Soft Materials (FUNSOM) & Collaborative Innovation Center of Suzhou Nano Science and Technology, Jiangsu Key Laboratory for Carbon-Based Functional Materials and Devices, Soochow University, Suzhou, Jiangsu 215123, China

Supporting Information

ABSTRACT: In the past few years, graphene and its derivative, graphene oxide (GO), have been extensively studied for their applications in biotechnology. In our previous work, we reported certain PEGylated GOs (GO-PEGs) can selectively promote trypsin activity and enhance its thermostability. To further explore this, here we synthesized a series of GO-PEGs with varying PEGylation degrees. Enzymatic activity assay shows that both GO and GO-PEGs can protect trypsin, but not chymotrypsin, from thermal denaturation at high temperature. Surprisingly, the lower the PEGylation degree, the better the protection, and GO as well as the GO-PEG with the lowest PEGylation degree show the highest protection efficiency (~70% retained activity at 70 °C). Fluorescence spectroscopy analysis shows that GO/GO-PEGs have strong interactions with trypsin. Molecular Dynamics (MD) simulation results reveal that trypsin is adsorbed onto the surface of GO through its cationic residues and hydrophilic residues. Different from chymotrypsin adsorbed on GO, the active site of trypsin is covered by GO. MD simulation at high temperature shows that, through such interaction with GO, trypsin's active site is therefore stabilized and protected by GO. Our work not only illustrates the promising potential of GO/GO-PEGs as efficient, selective modulators for trypsin, but also provides the interaction mechanism of GO with specific proteins at the nano–bio interface.

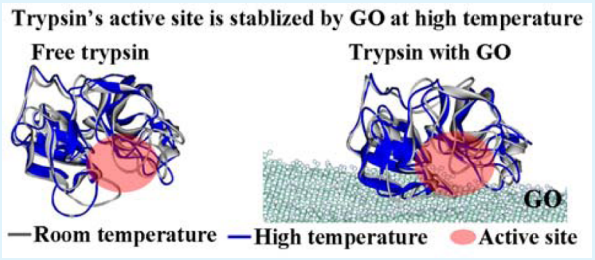

KEYWORDS: *graphene oxide, nano–bio interface, molecular dynamics simulation, enzyme thermostability, trypsin*

INTRODUCTION

Enzymes are essential for catalyzing reactions in living organisms such as digestion process, metabolism, gene expression, signal transduction, and immune responses. In addition, enzymes are biocatalysts extensively used in a wide range of industries and biomedical research.[1−3] However, when enzymes are used in operating environment, the exposure to temperature, ionic strength, and pH limits the application of enzymes. It is well-known that high temperature may lead to denatured structure of an enzyme resulting in loss of catalytic activity of the biocatalyst.[4] Therefore, it is imperative to develop methods to enhance the activity and thermostability of enzymes. Amino acid substitution has been used to enhance enzyme thermostability, but this method has not achieved much success in converting enzymes into thermo-stable enzymes.[5] Recently, along with the development of nanomaterials, various nanoparticles have been reported for improving the thermostabilities of enzymes,[6−9] yet mostly through an enzyme immobilization process. To efficiently immobilize an enzyme onto nanoparticle surfaces, a lot of work is required to functionalize the nanoparticle surface.[1,6−11] In addition, for most nanomaterials, it is hard to fully characterize their surface using conventional surface analytical tools alone, but when combined with Molecular Dynamics (MD) simulation tools, the data could provide more extensive understanding of the surface and the nano–bio interface, which is critical for biological effects and the rational design of functionalized nanomaterials.[1,12−16]

Graphene and its derivative graphene oxide (GO) have attracted tremendous attention due to their unique physical, chemical, and mechanical properties in the past several years.[17−19] GO possesses a single-layered, two-dimensional, sp^2 hybrid structure, having a large specific surface area with sufficient functional surface groups, which can provide an ideal platform for loading of small organic and biomacromolecules without any surface modification or any coupling reagents. These intriguing physical, chemical, and mechanical properties afford GO potential for wide applications in biotechnology and biomedicine. For instance, GO and functionalized GOs have been used for gene and small drug molecules delivery,[20−23] biosensing,[24−30] cancer therapeutics,[31−33] cellular imaging,[34,35] antibacterial agents,[36−39] as well as a modulator for enzymes.[1,40,41]

In our previous work, we uncovered that certain types of PEGylated graphene oxide (GO-PEG) were able to efficiently and selectively improve trypsin activity and protect it from thermal denaturation above 70 °C.[40] To further investigate the interactions between trypsin and GO/GO-PEG, we synthesized a series of GO-PEGs with varying PEGylation degrees (GO-

Received: April 10, 2015
Accepted: May 19, 2015
Published: May 19, 2015

DOI: 10.1021/acsami.5b03118
ACS Appl. Mater. Interfaces 2015, 7, 12270−12277

PEG-1, GO-PEG-2.5, and GO-PEG-5). Enzymatic activity assay shows that both GO and GO-PEGs can enhance thermostability of trypsin, but not chymotrypsin, and interestingly, GO and GO-PEG-1 (the one with the lowest PEGylation degree) show the highest protection efficiency. In addition, we use fluorescence spectroscopy and MD simulation to explore the interaction mechanism of GO with trypsin. Fluorescence spectroscopy analysis demonstrates that GO/GO-PEG strongly interacts with trypsin and changes the conformation of trypsin. MD simulation results reveal that trypsin is adsorbed onto the surface of GO through its cationic residues and hydrophilic residues during 35 ns MD simulations. Different from our previous MD simulation of chymotrypsin adsorbed on GO,[1] the active site of trypsin is covered by GO. MD simulation at high temperature shows that the active site of trypsin is stabilized by GO. Our work not only indicates the promising potential of GO/GO-PEGs as efficient, selective modulators for trypsin, but also provides more in-depth understandings of the interaction mechanism of GO with specific proteins at the nano−bio interface.

EXPERIMENTAL SECTION

Reagents. 10k-6*br*-PEG-NH_2 was purchased from Sunbio Inc. (South Korea). All other reagents and enzymes were purchased from Sigma-Aldrich (St. Louis, MO, USA).

Preparation and Characterization of GO and GO-PEGs. GO was synthesized from flake graphite following a slightly modified Hummer's method as previously described.[42,43] GO-PEG-1, GO-PEG-2.5, and GO-PEG-5 were prepared by conjugating GO with 10k-6*br*-PEG-NH_2 at feeding ratios of 1:1, 1:2.5, and 1:5 according to our method developed previously.[40] Briefly, to prepare GO-PEG-1, as-prepared GO solution (0.5 mg mL^{-1}) was mixed with 10k-6*br*-PEG-NH_2 (0.5 mg mL^{-1}) and sonicated with a water bath sonicator for 5 min. After the pH value of the reaction mixture was adjusted to ∼7.5 by using 1 M $NaHCO_3$ solution, the mixture was mixed with *N*-(3-(dimethylamino)propyl)-*N*′ ethylcarbodiimide hydrochloride (EDC) (0.5 mg mL^{-1}) and sonicated for another 15 min followed by a 30 min stirring at room temperature. Then, a second portion of EDC (1 mg mL^{-1}) was added, and the mixture was continuously stirred at room temperature for 2 h. After the third portion of EDC (1 mg mL^{-1}) was added, the mixture was stirred for another 3 h before being purified using an Amicon Ultra Centrifugal Filters with molecular weight cutoff (MWCO) of 100 kDa (Millipore, Ireland). Finally, the purified GO-PEG-1 was collected, resuspended in water, and stored at 4 °C for the following experiments. GO-PEG-2.5 and GO-PEG-5 were prepared using the same procedures for the synthesis of GO-PEG-1 except that 1.25 mg mL^{-1} and 2.5 mg mL^{-1} of 10k-6*br*-PEG-NH_2 were used, respectively.

The concentrations of as-prepared GO and GO-PEGs were quantified by utilizing their corresponding absorbance at 230 nm with a mass extinction coefficient of 65 mL mg^{-1} cm^{-1}.[40] Atomic force microscopy (AFM, MutiMode V, Veeco) was exploited to visualize the morphologies and evaluate the thicknesses of as-prepared GO and GO-PEGs. The Fourier transform infrared (FT-IR) spectrum, zeta potentials, and dynamic light scattering (DLS) sizes of GO and GO-PEGs were recorded with a Hyperion series FT-IR spectrometer (Bruker) and DLS on a Zen3690 (Malvern) at the scattering angle θ = 17°. The PEG contents in GO-PEG-1, GO-PEG-2.5, and GO-PEG-5 were estimated to be 34.5%, 60.5%, and 65.7%, respectively, using thermogravimetric analysis (TGA) as previously reported.[40]

Enzymatic Activity Assay. The catalytic activity of trypsin on urea-denatured substrate hemoglobin (Hb) was carried out with a modified spectrophotometric method.[40] Briefly, trypsin (20 μg mL^{-1}) was preincubated with either water (as control), GO, or different GO-PEGs (40 μg mL^{-1} in terms of GO) in water at room temperature for 16 min, respectively. Then, the mixtures were mixed with same volume of urea-denatured Hb dissolved in 20 mM phosphate buffered saline (PBS; pH 8.0) to make an ultimate Hb concentration of 2.5 mg mL^{-1}, and incubated at 40 °C for 10 min, respectively. After that, the digestion reaction was terminated by using 0.2 M trichloroacetic acid. The amount of digestion products was quantified by the Lowry method.[44]

For the thermostability test, trypsin was preincubated with water (as control), GO, or GO-PEGs at room temperature for 16 min as aforementioned. Then, the mixture suspension was incubated with a metal bath at 70 °C for 5 min (or prolonged incubation time as indicated in Supporting Information, Figure S2) and then kept on ice; the residual trypsin activity was determined as described above.

To study the influence of GO and GO-PEGs on the enzymatic activity and thermostability of chymotrypsin, the same method for trypsin as aforementioned was exploited except that 10 μg mL^{-1} of chymotrypsin was used in the experiments.

Blocking the Terminal Amino Groups of GO-PEG-5. To block the terminal amino groups of GO-PEG-5, GO-PEG-5 (0.2 mg mL^{-1}) was incubated with 6% (v/v) of acetic anhydride (AA) in 20 mM PBS containing 30 mM $NaHCO_3$ and 20 mM EDC at room temperature for 4 h. Then, the $NaHCO_3$ was added to mixture suspension to adjust the pH to 8.0, and additional EDC was added to reach a final concentration of 25 mM. Unconjugated AA was removed by filtration using Amicon Ultra Centrifugal Filters (MWCO = 100 kDa) as described above.

Fluorescence Spectroscopy to Study Enzyme Secondary Structure. To investigate the effect of GO and GO-PEGs on enzyme secondary structure, the enzyme (0.1 mg mL^{-1} trypsin or 0.05 mg mL^{-1} chymotrypsin) was preincubated with either water, 10k-6*br*-PEG-NH_2 (0.25 mg mL^{-1}), GO, or GO-PEGs (0.05 mg mL^{-1} in terms of GO) at room temperature for 16 min, then kept at room temperature, or subjected to thermal treatment in a metal bath at 70 °C, for 5 min. The fluorescence spectrum of each sample was measured (excitation, 290 nm; emission spectrum recorded, 300−560 nm).[45]

Molecular Dynamics Simulations. In our study, all MD simulations were performed by the NAMD molecular dynamic software package[46] with the CHARMM27 force field.[47] The Dreiding force field was applied to parametrize the GO.[1,48] The native structure of trypsin was obtained from the Protein Data Bank (PDB: 1S5S[49]) and was prepared using the Discover Studio2.5 (6) for geometry optimization.

The GO sheet was prepared with a size of 10.0 × 9.0 nm^2 (3115 carbon atoms), which provided a sufficiently large surface for adsorption of trypsin. The epoxy and hydroxyl groups are randomly grafted to the carbon atoms on the GO basal plane. The carboxyl groups are attached to the carbon atoms on the edge randomly. The GO model considered here is not completely oxidized: $C_{10}O_1(OH)_1$ (one epoxy group and one hydroxyl group per 10 carbon atoms are attached to the GO basal plane), which reflects a typical outcome from a standard oxidation process.[1,50−53]

In the initial configuration of the MD simulations, the GOs were aligned in the *x*−*y* plane, while trypsins were separated by ∼13 Å vertically along the *z* direction. Then, the combinations were embedded into a rectangular box of TIP3P water molecules.[54] Periodic boundary conditions were applied in all three directions. During all simulations, the GOs were fixed all the time. The particle mesh Ewald (PME) summation[55] was applied to model the full-system electrostatic interactions, with a cutoff of 12 Å for the separation of the direct and reciprocal space summation. Also, the SWITCH algorithm, with a cutoff distance of 12 Å, was applied to calculate van der Waals forces. The NPT ensemble was used for all systems where the Langevin's piston and the Nose−Hoover thermostat were applied, respectively, to keep the pressure at 1 bar the temperature at 310 and 380 K.[56]

RESULTS AND DISCUSSION

Preparation and Functionalization of GO Nanosheets. GO was synthesized from graphite following the modified Hummer's method.[42,43] Three types of GO-PEGs with

DOI: 10.1021/acsami.5b03118
ACS Appl. Mater. Interfaces 2015, 7, 12270−12277

increasing PEGylation degrees (GO-PEG-1, GO-PEG-2.5, and GO-PEG-5) were prepared from GO sheets by covalent conjugation with indicated amounts of 10k-6*br*-PEG-NH_2 via amide formation as previously described.[40] Both the zeta potential and FT-IR spectra of GO and GO-PEGs (Table 1 and Supporting Information, Figure S1) suggested that 10k-6*br*-PEG-NH_2 had been successfully covalently conjugated with GO. AFM images showed that GO/GO-PEGs were mainly single or double layered. The size of GO was a few micrometers, whereas after PEGylation, the GO-PEGs were much smaller with a size less than 50 nm (Figure 1a). As shown in Figure 1, panel b, the majority of GO precipitated out after centrifugation in PBS at 21 000*g* for 5 min, while no noticeable aggregation of GO-PEGs could be observed after centrifugation under the same conditions, suggesting greatly improved dispersibility in physiological solutions after PEGylation.

Table 1. Zeta Potentials of GO and GO-PEGs

sample	zeta potential (mV)
GO	−41.3 ± 1.39
GO-PEG-1	−22.6 ± 2.55
GO-PEG-2.5	−15.2 ± 0.86
GO-PEG-5	−9.1 ± 1.13
GO-PEG-5-AA	−16.5 ± 1.52

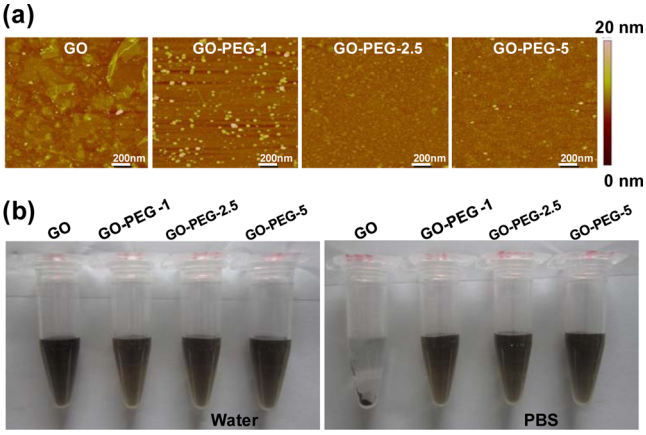

Figure 1. GO and GO-PEGs used in the study: (a) AFM images; (b) dispersibilities in water and PBS, photos were taken after centrifugation at 21 000*g* for 5 min.

GO Enhances Thermostability of Trypsin Selectively. We first investigated the effect of GO on the thermostability of trypsin using hemoglobin as substrate. As shown in Figure 2, panel a, free trypsin quickly denatured at 70 °C, resulting in less than 10% of the enzyme activity retained. Although preincubation of trypsin with GO showed some inhibitory effect on trypsin activity at room temprature (25 °C), little further decrease of the enzyme activity was observed after thermal treatment at 70 °C for 5 min, that is, nearly 70% of trypsin activity was retained in the presence of GO. Furthermore, GO was able to efficiently protect trypsin during prolonged thermal treatment. As shown in Supporting Information, Figure S2, in the presence of GO, even after incubation at 70 °C for 50 min, only a slight reduction in trypsin activity was observed, and over 50% of trypsin activity could be retained.

Trypsin is a typical serine protease belonging to a large protein family. Therefore, we also investigated the effect of GO on another typical serine protease, chymotrypsin, a subfamily member closely related to trypsin with similar tertiary structures and catalytic mechanisms.[57] As shown in Figure 2, panel b, GO significantly inhibited the activity of chymotrypsin and did not protect chymotrypsin against thermal denaturation. The distinct effects of GO on trypsin and chymotrypsin indicate that GO can enhance trypsin's thermostability selectively.

Degrees of PEGylation on GO Affect Its Ability to Protect Trypsin Against Thermal Denaturation. In our previous work, we discovered that GO-PEG-5 could selectively enhance trypsin's thermostability.[40] Given the above finding that GO could also enhance trypsin's thermostability, the first question arose as whether the PEGylation degree plays a role. Therefore, the effects of GO-PEGs with increasing PEGylation degrees (GO-PEG-1, GO-PEG-2.5, and GO-PEG-5) on the thermostability of trypsin were analyzed accordingly. As shown in Figure 2c, all three GO-PEGs could protect trypsin against thermal denaturation to certain extents, but the highest protection efficiency was obtained with as-made GO and GO-PEG-1, and the protection efficiency decreased with increasing PEGylation degree on GO surface.

Since the coating polymer 10k-6*br*-PEG-NH_2 itself has no effect on trypsin (Supporting Information, Figure S3a), the fact that the degree of PEGylation can affect GO/GO-PEGs' abilities to protect trypsin is likely due to the alterations on the GO surface by PEGylation. One important alteration after PEGylation is the decrease in the amount of carboxyl groups and the introduction of a number of positively charged NH_2 groups onto the negatively charged GO surface, leading to an increase in the surface charge (Table 1). To investigate any roles of surface charge in the interaction between GO/GO-PEGs and trypsin, the terminal NH_2 groups of GO-PEG-5 were partially blocked by acetic anhydride, producing GO-PEG-5-AA. The surface charge of GO-PEG-5-AA decreased to an extent similar to that of GO-PEG-2.5, coinciding with an increase in the former's ability to stabilize trypsin at high temperature to a level comparable with the latter's (Table 1 and Figure 2c), indicating the involvement of surface charge in the interaction between GO/GO-PEGs and trypsin.

Effects of GO/GO-PEGs on the Structure of Trypsin. Change of enzyme activity usually correlates with change in its secondary structure. The effect of GO/GO-PEGs on the secondary structure of trypsin was investigated by fluorescence spectroscopy. Trypsin contains chromophoric residues including tryptophan, tyrosine, and phenylalanine. Any structural changes causing exposure of the chromophoric residues to the aqueous environment will result in a red-shift and can be analyzed by fluorescence spectroscopy.[41] As shown in Figure 3, natural trypsin has a characteristic fluorescence emission peak at 343 nm (black line),[45] while thermal denaturation of trypsin resulted in a red-shift to 358 nm (red line). The coating polymer, PEG, showed no effect on trypsin's structure, demonstrated by the almost identical fluorescence spectra of trypsin in the absence and in the presence of 10k-6*br*-PEG-NH_2 (Supporting Information, Figure S3b), consistent with the corresponding enzymatic activity data (Supporting Information, Figure S3a).

In contrast, preincubation of trypsin with GO or GO-PEG-1 led to the red-shift of trypsin's fluorescence emission peak to 362 nm (Figure 3a,b, green line), which is indication of strong

DOI: 10.1021/acsami.5b03118
ACS Appl. Mater. Interfaces 2015, 7, 12270−12277

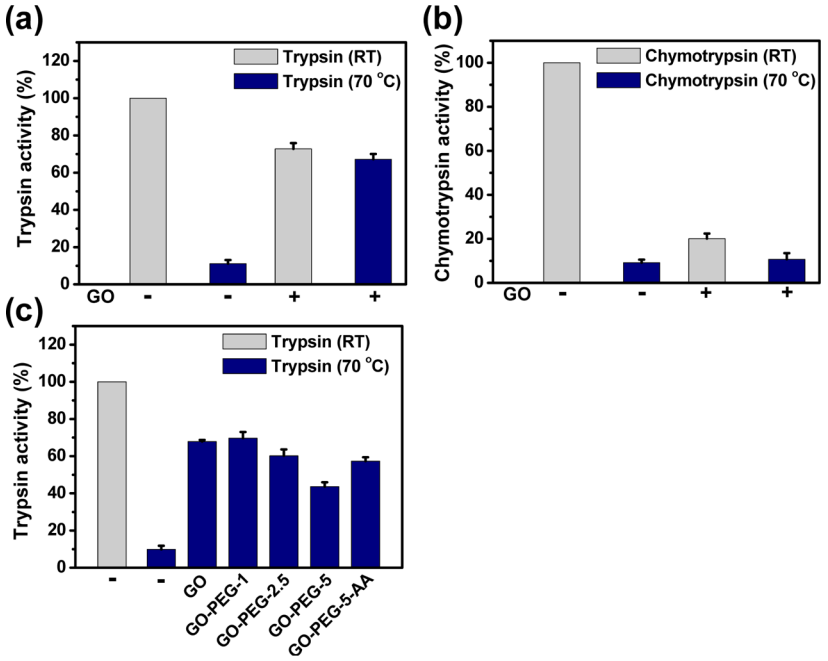

Figure 2. Effects of GO and GO-PEGs on enzymes' thermostabilities. (a) Trypsin and (b) chymotrypsin were preincubated with GO, and the enzyme activities retained before and after thermal treatment were analyzed. (c) Trypsin was preincubated with GO or GO-PEGs as indicated, and the enzyme activities retained after thermal treatment were analyzed. Error bars represent the standard deviations ($n \geq 3$).

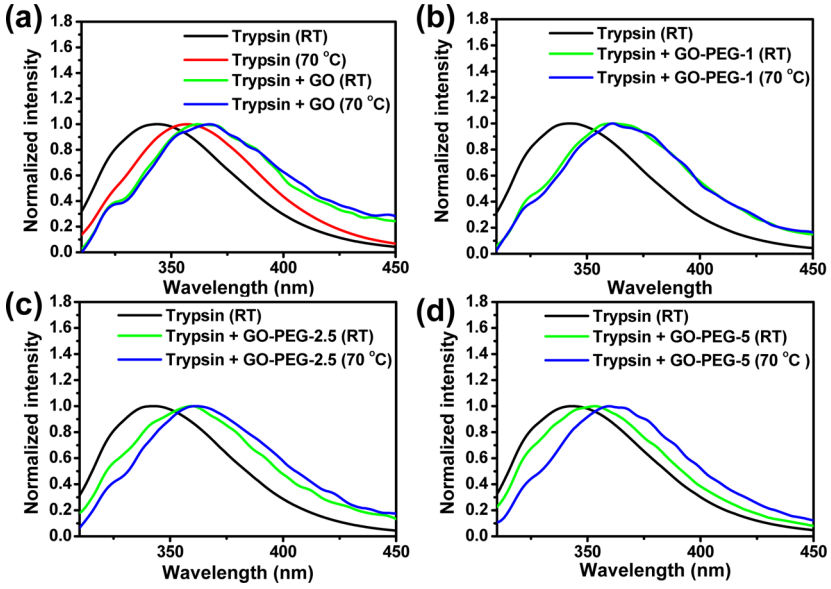

Figure 3. Fluorescence spectroscopy analysis of trypsin. Trypsin was preincubated with either (a) GO, (b) GO-PEG-1, (c) GO-PEG-2.5, or (d) GO-PEG-5, and the fluorescence spectrum of each sample was measured before (room temperature, RT) and after thermal treatment (70 °C). The spectra of natural trysin before and after thermal treatment were recorded as well. Excitation: 290 nm.

interaction between GO/GO-PEG-1 and trypsin. Correlating with the enzymatic activity data in Figure 2, panels a and c, in the presence of GO or GO-PEG-1, thermal treatment did not further affect trypsin's fluorescence spectra (Figure 3a,b, compare the blue lines with the green lines), which suggests that, at high temperature, the structure of trypsin could be stabilized by its interaction with GO/GO-PEG-1.

The other two GO-PEGs (GO-PEG-2.5 and GO-PEG-5) also showed strong interactions with trypsin, suggested by the red-shifts of trypsin's fluorescence emission peak after preincubation with them (Figure 3c,d, green lines). However, compared with GO and GO-PEG-1 (peak at 362 nm), GO-PEG-2.5 induced a smaller red-shift (peak at 359 nm), while GO-PEG-5 induced the smallest red-shift among them (peak at 353 nm), indicating that the higher the PEGylation degree, the weaker the interaction with trypsin. This might explain the observation that, unlike GO and GO-PEG-1, which could efficiently protect trypsin's structure during thermal treatment (Figure 3a,b), GO-PEG-2.5 and GO-PEG-5 showed reduced abilities to preserve trypsin's structure at high temperature (Figure 3c,d). In the presence of GO-PEG-2.5, thermal treatment at 70 °C led to a further red-shift in trypsin's emission spectra, whereas in the case of GO-PEG-5, an even larger red-shift in trypsin's fluorescence spectra was induced by

DOI: 10.1021/acsami.5b03118
ACS Appl. Mater. Interfaces 2015, 7, 12270−12277

thermal treatment (Figure 3c,d, compare the blue lines with the green lines), indicating the lowest thermo-protection efficiency of GO-PEG-5. All the fluorescence spectra data correlate well with the enzymatic activity data shown in Figure 2.

MD Simulation Reveals that the Active Site of Trypsin is Covered by GO. To further investigate the interaction mechanism of GO with trypsin, we performed all-atom MD simulation for GO and trypsin in explicit water solvent. Figure 4, panel a shows the initial structures of the simulated system.

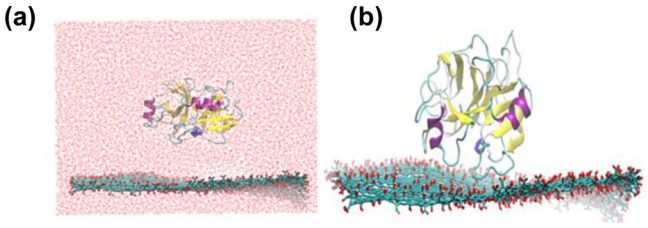

Figure 4. MD simulation of adsorption of trypsin onto GO. (a) The MD simulation box of trypsin-GO embedded in water at room temperature, showing the initial structures of the simulated system. (b) After 35 ns of MD simulation, trypsin is absorbed onto GO and shows strong interactions with GO. Water molecules are not shown in panel b.

After 35 ns of dynamic simulation, trypsin was absorbed onto GO surface (Figure 4b), and the system equilibrates as RMSD converges toward 3.5 Å (Figure 5b). It indicates that GO has strong interaction with trypsin, which changes the conformations of chromophores residues of trypsin, as shown in Figure 5, panel c (the chromophores residues are colored in red in Figure 5c).

The α-helices changed slightly (the content of α-helix reduced from 9.01% to 6.76%), while the random coils of trypsin fluctuate sharply, which can be observed easily in Figure 5, panel a. In the final configuration after MD (Figure 5c), the active site of trypsin is covered by GO, and residues of active site interact with the functional groups in GO surface. Thus, the activity of trypsin would be affected, consistent with the enzymatic activity assay results in Figure 2, panel a.

By analyzing the trajectory of our MD results, we find that several positively charged or polar residues induce the adsorption by interacting with GO. These residues within 5 Å of GO after 35 ns of MD are listed in Supporting Information, Table S1. Among them, Lys43, Lys200, Lys202 are positively charged residues, and Gln198, Thr72, Thr80, Thr152, and Thr155 are polar residues. These charged residues and polar residues have strong coulomb interactions with negatively charged groups on the GO surface.

There are three types of residues responsible for fluorescence in protein, namely Trp, Tyr, and Phe. As shown in Figure 5, panel c, the chromophoric residues in trypsin are displayed in red, among which, Tyr42 and Phe76 are found to closely interact with GO, showing strong hydrophobic interaction with GO. Besides Tyr42 and Phe76, there are more hydrophobic residues (highlighted in blue) interacting with GO strongly, as shown in Figure 5, panel c. Our MD results indicate the change of chromophoric residues, which is consistent with the fluorescence spectroscopy analysis in Figure 3, panel a.

Stabilization of Trypsin's Active Site by GO at High Temperature. To further explore the mechanism of how GO enhances the thermostability of trypsin, we performed MD simulations for trypsin with GO at high temperature (368 K). In parallel, MD results for trypsin only and trypsin interacting with GO are compared.

The alignments of trypsin structure at room temperature (gray) and those at high temperature (blue) after MD simulations without or with GO are shown in Figure 6, panels a and b, respectively. By analyzing the structures, we find that, in the absence of GO, the loop part of the active site of trypsin undergoes significant conformational change at high temperature (Figure 6a), whereas in the presence of GO, it interacts with GO strongly and keeps stable at high temperature (Figure 6b). Figure 6, panel c shows time evolution of RMSD of the active site of trypsin at high temperature. For trypsin-only trajectory, it shows big RMSD values (black line), while for

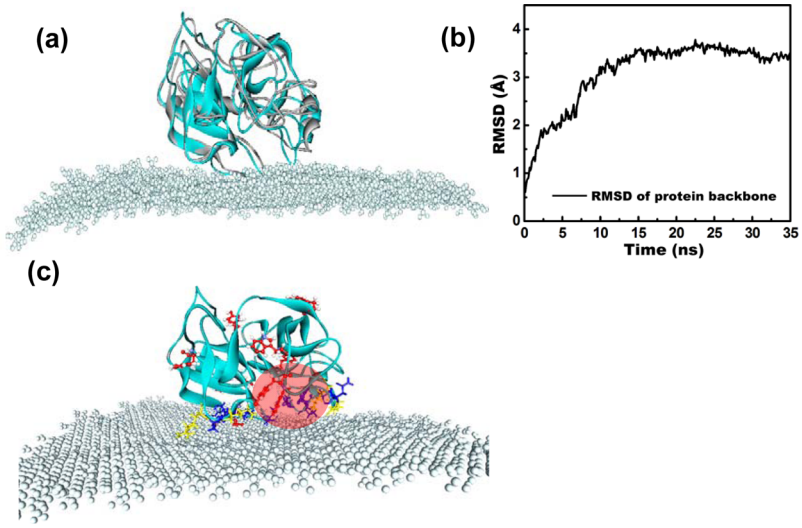

Figure 5. MD simulation reveals that the active site of trypsin is covered by GO. (a) Superposition of trypsin (cyan) after 35 ns of MD simulation with the crystal structure (Gray). (b) The changes of RMSD values of backbone atoms of trypsin, which indicates that GO has a strong interaction with trypsin. (c) Trypsin interacts strongly with GO. The yellow residues are positively charged residues absorbed on GO, which show strong coulomb interactions with GO. The blue residues are neutral residues absorbed on GO, which show strong van de Waals interactions with GO. The red residues are chromophores of trypsin. The active site of trypsin is highlighted by the red sphere.

DOI: 10.1021/acsami.5b03118
ACS Appl. Mater. Interfaces 2015, 7, 12270−12277

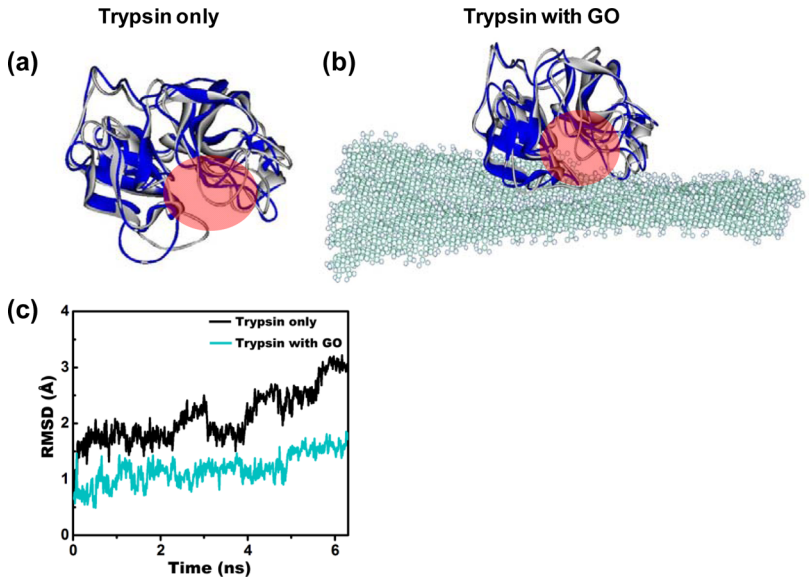

Figure 6. Stabilization of trypsin's active aite by GO at high temperature. (a) The active site of trypsin (the sphere colored in red) is deformed after MD at high temperature. (b) The active site of trypsin with GO is stable after MD at high temperature. The structure of trypsin at room temperature is shown in gray, and the structure of trypsin at high temperature is shown in blue. (c) Time evolution of RMSD indicates that the active site of trypsin at high temperature shows larger RMSD values (black line) than did it absorbed onto GO (blue line).

trypsin with GO trajectory, it shows small RMSD values (dark blue line), indicating that GO could stabilize the active site of trypsin at high temperature.

Critical Surface Functional Groups at the Nano–Bio Interface. MD simulation, when correlated with experimental data, can provide useful information for interaction mechanisms between proteins and nanomaterials.[1,41,58−60] In our case, the MD results shown above, which are consistent with the enzyme activity data and fluorescence spectroscopy data, not only suggest that GO could enhance the thermostability of trypsin, but also provide the in-depth mechanism of how GO interacts with trypsin and enhances trypsin's thermostability. The fluorescence spectroscopy data, which show that preincubation of trypsin with GO resulted in the red-shift of trypsin's fluorescence emission peak to 362 nm (Figure 3a, green line), clearly indicate strong interactions between GO and trypsin and are consistent with the MD results (Figures 5 and 6). The MD results also show that GO's surface covers the active site of trypsin and keeps the active site stable at high temperature, corroborating with the enzymatic activity data (Figure 2a) and the secondary structure analysis using fluorescence spectroscopy (Figure 3a). Since trypsin interacts with negatively charged groups on the GO surface through its cationic residues and hydrophilic residues, PEGylation of the GO surface would alter the surface charge significantly (Table 1). This alteration of the GO surface would thus impair GO-PEGs' interactions with trypsin, and the higher the PEGylation degree, the weaker the interaction, resulting in descending thermo-protection efficiencies of GO-PEG-1, GO-PEG-2.5, and GO-PEG-5 for trypsin (Figures 2c and 3b−d). Blocking of the terminal amino groups with acetic anhydride of GO-PEG-5 decreases the surface charge of GO-PEG-5-AA to an extent similar to that of GO-PEG-2.5, and both nanosheets show comparable abilities in stabilizing trypsin at high temperature (Table 1 and Figure 2c), further indicating the important roles of surface functional groups at the nano−bio interface.

Trypsin and chymotrypsin are two closely related serine proteases in the same subfamily, but they interact with GO differently. According to the above MD results and the MD results from our previous work,[1] which investigated the interacting mechanism of chymotrypsin with GO, both enzymes form strong interactions with GO through their cationic residues and hydrophilic residues. However, because of the unique distributions of these residues surrounding their active sites, they interact with GO differently and thus lead to opposite outcomes. In the case of trypsin, its interaction with GO results in the covering of its active site by GO (Figure 5). Although this interaction slightly changes the conformation of the active site of trypsin, causing mild decrease of trypsin activity, more importantly, it serves as a stabilizer at high temperature, greatly enhancing the thermostability of trypsin (Figures 2a and 6). In contrast, chymotrypsin's interaction with GO results in the deformation of its active site,[1] leading to severe inhibition of enzyme activity with no thermo-protection at all (Figure 2b and Supporting Information, Figure S4). This demonstrates that, in addition to the functional groups on GO surface, the surface groups on the other interacting partner (enzyme) also contribute largely to the interaction and the selectivity.

CONCLUSION

In this work, we studied the interactions of GO and GO-PEGs with two closely related enzymes, trypsin and chymotrypsin, and discovered that GO/GO-PEGs could selectively stabilize trypsin, but not chymotrypsin, at high temperature. Enzymatic activity assay also suggests that the PEGylation degree of the GO nanosheets could affect their abilities to enhance thermostability of trypsin, with GO and GO-PEG-1 (the one with the lowest PEGylation degree) possessing the highest protection efficiency (~70% retained enzyme activity at 70 °C). The fluorescence spectroscopy analysis and MD simulations demonstrate the strong interactions between GO/GO-PEGs and trypsin. MD simulations reveal that trypsin is adsorbed onto the surface of GO through its cationic residues and hydrophilic residues; the active site of trypsin is covered by GO and is stabilized by GO at high temperature. The selectivity of

DOI: 10.1021/acsami.5b03118
ACS Appl. Mater. Interfaces 2015, 7, 12270−12277

GO toward trypsin is caused by the different effects of GO on the conformations of trypsin and chymotrypsin. Our work not only demonstrates the promising potential of GO/GO-PEGs as efficient, selective modulators for trypsin, further promoting their potential applications in enzyme engineering and enzyme-based applications, but also provides the interaction mechanism of GO with specific proteins at the nano−bio interface, which sheds light on the rational design of functionalized nanomaterials.

■ ASSOCIATED CONTENT

Supporting Information

FT-IR data and TGA data of GO and GO-PEGs; prolonged thermo-protection of trypsin by GO; effects of coating polymer 10k-6*br*-PEG-NH_2 on trypsin's thermostability and secondary structure; effects of GO on chymotrypsin's secondary structure; residues of trypsin within 5 Å of GO after 35 ns MD simulation. The Supporting Information is available free of charge on the ACS Publications website at DOI: 10.1021/acsami.5b03118.

■ AUTHOR INFORMATION

Corresponding Authors

*Phone: +86-0512-65880947. Fax: +86-0512-65880820. E-mail: rpeng@suda.edu.cn.

*Phone: +86-0512-65882037. Fax: +86-0512-65880820. E-mail: yyli@suda.edu.cn.

Notes

The authors declare no competing financial interest.

■ ACKNOWLEDGMENTS

This work was supported by the National Basic Research Program of China (973 Program, Grant Nos. 2012CB932600 and 2012CB932400), the National Natural Science Foundation of China (Grant Nos. 91233115, 21273158, and 91227201), and a project funded by the Priority Academic Program Development of Jiangsu Higher Education Institutions (PAPD). Additional support came from the Fund for Innovative Research Teams of Jiangsu Higher Education Institutions, Collaborative Innovation Center of Suzhou Nano Science and Technology.

■ REFERENCES

(1) Sun, X.; Feng, Z.; Hou, T.; Li, Y. Mechanism of Graphene Oxide as an Enzyme Inhibitor from Molecular Dynamics Simulations. *ACS Appl. Mater. Interfaces* **2014**, *6*, 7153−7163.

(2) Kirk, O.; Borchert, T. V.; Fuglsang, C. C. Industrial Enzyme Applications. *Curr. Opin. Biotechnol.* **2002**, *13*, 345−351.

(3) Xin, L.; Zhou, C.; Yang, Z.; Liu, D. Regulation of an Enzyme Cascade Reaction by a DNA Machine. *Small* **2013**, *9*, 3088−3091.

(4) Cherry, J. R.; Fidantsef, A. L. Directed Evolution of Industrial Enzymes: An Update. *Curr. Opin. Biotechnol.* **2003**, *14*, 438−443.

(5) Imanaka, T.; Shibazaki, M.; Takagi, M. A New Way of Enhancing the Thermostability of Proteases. *Nature* **1986**, *324*, 695−697.

(6) Li, D.; He, Q.; Cui, Y.; Duan, L.; Li, J. Immobilization of Glucose Oxidase onto Gold Nanoparticles with Enhanced Thermostability. *Biochem. Biophys. Res. Commun.* **2007**, *355*, 488−493.

(7) Li, J.; Wang, J.; Gavalas, V. G.; Atwood, D. A.; Bachas, L. G. Alumina-Pepsin Hybrid Nanoparticles with Orientation-Specific Enzyme Coupling. *Nano Lett.* **2003**, *3*, 55−58.

(8) Li, C.; Huang, M.; Gu, Z.; Hong, Y.; Cheng, L.; Li, Z. Nanosilica Sol Leads to Further Increase in Polyethylene Glycol (PEG) 1000-Enhanced Thermostability of β-Cyclodextrin Glycosyltransferase from *Bacillus circulans*. *J. Agric. Food Chem.* **2014**, *62*, 2919−2924.

(9) Kao, K.-C.; Lin, T.-S.; Mou, C.-Y. Enhanced Activity and Stability of Lysozyme by Immobilization in the Matching Nanochannels of Mesoporous Silica Nanoparticles. *J. Phys. Chem. C* **2014**, *118*, 6734−6743.

(10) Lin, Y.; Lu, F.; Tu, Y.; Ren, Z. Glucose Biosensors Based on Carbon Nanotube Nanoelectrode Ensembles. *Nano Lett.* **2004**, *4*, 191−195.

(11) Chen, N.; Wang, H.; Huang, Q.; Li, J.; Yan, J.; He, D.; Fan, C.; Song, H. Long-Term Effects of Nanoparticles on Nutrition and Metabolism. *Small* **2014**, *10*, 3603−3611.

(12) Ge, C.; Du, J.; Zhao, L.; Wang, L.; Liu, Y.; Li, D.; Yang, Y.; Zhou, R.; Zhao, Y.; Chai, Z.; Chen, C. Binding of Blood Proteins to Carbon Nanotubes Reduces Cytotoxicity. *Proc. Natl. Acad. Sci. U. S. A.* **2011**, *108*, 16968−16973.

(13) Guo, J.; Li, J.; Zhang, Y.; Jin, X.; Liu, H.; Yao, X. Exploring the Influence of Carbon Nanoparticles on the Formation of β-Sheet-Rich Oligomers of $IAPP_{22-28}$ Peptide by Molecular Dynamics Simulation. *PLoS One* **2013**, *8*, e65579.

(14) Kong, X.; Pan, P.; Li, D.; Tian, S.; Li, Y.; Hou, T. Importance of Protein Flexibility in Ranking Inhibitor Affinities: Modeling the Binding Mechanisms of Piperidine Carboxamides as Type I1/2 ALK Inhibitors. *Phys. Chem. Chem. Phys.* **2015**, *17*, 6098−6113.

(15) Sun, H.; Tian, S.; Zhou, S.; Li, Y.; Li, D.; Xu, L.; Shen, M.; Pan, P.; Hou, T. Revealing the Favorable Dissociation Pathway of Type II Kinase Inhibitors via Enhanced Sampling Simulations and Two-End-State Calculations. *Sci. Rep.* **2015**, *5*, 8457.

(16) Xi, L.; Li, S.; Yao, X.; Wei, Y.; Li, J.; Liu, H.; Wu, X. a In Silico Study Combining Docking and QSAR Methods on a Series of Matrix Metalloproteinase 13 Inhibitors. *Arch. Pharm. Chem. Life Sci.* **2014**, *347*, 825−833.

(17) Stankovich, S.; Dikin, D. A.; Dommett, G. H. B.; Kohlhaas, K. M.; Zimney, E. J.; Stach, E. A.; Piner, R. D.; Nguyen, S. T.; Ruoff, R. S. Graphene-Based Composite Materials. *Nature* **2006**, *442*, 282−286.

(18) Geim, A. K.; Novoselov, K. S. The Rise of Graphene. *Nat. Mater.* **2007**, *6*, 183−191.

(19) Yang, K.; Li, Y.; Tan, X.; Peng, R.; Liu, Z. Behavior and Toxicity of Graphene and Its Functionalized Derivatives in Biological Systems. *Small* **2013**, *9*, 1492−1503.

(20) Feng, L. Z.; Zhang, S.; Liu, Z. Graphene Based Gene Transfection. *Nanoscale* **2011**, *3*, 1252−1257.

(21) Zhang, L.; Lu, Z.; Zhao, Q.; Huang, J.; Shen, H.; Zhang, Z. Enhanced Chemotherapy Efficacy by Sequential Delivery of siRNA and Anticancer Drugs Using PEI-Grafted Graphene Oxide. *Small* **2011**, *7*, 460−464.

(22) Liu, Z.; Robinson, J. T.; Sun, X.; Dai, H. PEGylated Nanographene Oxide for Delivery of Water-Insoluble Cancer Drugs. *J. Am. Chem. Soc.* **2008**, *130*, 10876−10877.

(23) Zhang, L.; Xia, J.; Zhao, Q.; Liu, L.; Zhang, Z. Functional Graphene Oxide as a Nanocarrier for Controlled Loading and Targeted Delivery of Mixed Anticancer Drugs. *Small* **2010**, *6*, 537−544.

(24) Balapanuru, J.; Yang, J. X.; Xiao, S.; Bao, Q.; Jahan, M.; Polavarapu, L.; Wei, J.; Xu, Q. H.; Loh, K. P. A Graphene Oxide−Organic Dye Ionic Complex with DNA-Sensing and Optical-Limiting Properties. *Angew. Chem., Int. Ed.* **2010**, *122*, 6699−6703.

(25) Zhou, M.; Zhai, Y.; Dong, S. Electrochemical Sensing and Biosensing Platform Based on Chemically Reduced Graphene Oxide. *Anal. Chem.* **2009**, *81*, 5603−5613.

(26) Zhang, Z.; Luo, L.; Chen, G.; Ding, Y.; Deng, D.; Fan, C. Tryptamine Functionalized Reduced Graphene Oxide for Label-Free DNA Impedimetric Biosensing. *Biosens. Bioelectron.* **2014**, *60*, 161−166.

(27) Wu, L.; Wang, J.; Yin, M.; Ren, J.; Miyoshi, D.; Sugimoto, N.; Qu, X. Reduced Graphene Oxide Upconversion Nanoparticle Hybrid for Electrochemiluminescent Sensing of a Prognostic Indicator in Early-Stage Cancer. *Small* **2014**, *10*, 330−336.

(28) Yin, S.; Wu, Y. L.; Hu, B.; Wang, Y.; Cai, P.; Tan, C. K.; Qi, D.; Zheng, L.; Leow, W. R.; Tan, N. S.; Chen, X. Three-Dimensional

DOI: 10.1021/acsami.5b03118
ACS Appl. Mater. Interfaces 2015, 7, 12270−12277

Graphene Composite Macroscopic Structures for Capture of Cancer Cells. *Adv. Mater. Interfaces* **2014**, *1*, 1300043.
(29) Ang, P. K.; Chen, W.; Wee, A. T. S.; Loh, K. P. Solution-Gated Epitaxial Graphene as pH Sensor. *J. Am. Chem. Soc.* **2008**, *130*, 14392−14393.
(30) Zhu, B.; Niu, Z.; Wang, H.; Leow, W. R.; Wang, H.; Li, Y.; Zheng, L.; Wei, J.; Huo, F.; Chen, X. Microstructured Graphene Arrays for Highly Sensitive Flexible Tactile Sensors. *Small* **2014**, *10*, 3625−3631.
(31) Yang, K.; Zhang, S.; Zhang, G.; Sun, X.; Lee, S.-T.; Liu, Z. Graphene in Mice: Ultrahigh in Vivo Tumor Uptake and Efficient Photothermal Therapy. *Nano Lett.* **2010**, *10*, 3318−3323.
(32) Robinson, J. T.; Tabakman, S. M.; Liang, Y.; Wang, H.; Sanchez Casalongue, H.; Vinh, D.; Dai, H. Ultrasmall Reduced Graphene Oxide with High Near-Infrared Absorbance for Photothermal Therapy. *J. Am. Chem. Soc.* **2011**, *133*, 6825−6831.
(33) Zhou, H.; Zhang, B.; Zheng, J.; Yu, M.; Zhou, T.; Zhao, K.; Jia, Y.; Gao, X.; Chen, C.; Wei, T. The Inhibition of Migration and Invasion of Cancer Cells by Graphene via the Impairment of Mitochondrial Respiration. *Biomaterials* **2014**, *35*, 1597−1607.
(34) Wang, Y.; Li, Z.; Hu, D.; Lin, C.-T.; Li, J.; Lin, Y. Aptamer/Graphene Oxide Nanocomplex for in Situ Molecular Probing in Living Cells. *J. Am. Chem. Soc.* **2010**, *132*, 9274−9276.
(35) Gollavelli, G.; Ling, Y.-C. Multi-Functional Graphene as an in Vitro and in Vivo Imaging Probe. *Biomaterials* **2012**, *33*, 2532−2545.
(36) Hu, W.; Peng, C.; Luo, W.; Lv, M.; Li, X.; Li, D.; Huang, Q.; Fan, C. Graphene-Based Antibacterial Paper. *ACS Nano* **2010**, *4*, 4317−4323.
(37) Tu, Y.; Lv, M.; Xiu, P.; Huynh, T.; Zhang, M.; Castelli, M.; Liu, Z.; Huang, Q.; Fan, C.; Fang, H.; Zhou, R. Destructive Extraction of Phospholipids from *Escherichia coli* Membranes by Graphene Nanosheets. *Nat. Nanotechnol.* **2013**, *8*, 594−601.
(38) Tian, T.; Shi, X.; Cheng, L.; Luo, Y.; Dong, Z.; Gong, H.; Xu, L.; Zhong, Z.; Peng, R.; Liu, Z. Graphene-Based Nanocomposite as an Effective, Multifunctional, and Recyclable Antibacterial Agent. *ACS Appl. Mater. Interfaces* **2014**, *6*, 8542−8548.
(39) Tang, J.; Chen, Q.; Xu, L.; Zhang, S.; Feng, L.; Cheng, L.; Xu, H.; Liu, Z.; Peng, R. Graphene Oxide−Silver Nanocomposite as a Highly Effective Antibacterial Agent with Species-Specific Mechanisms. *ACS Appl. Mater. Interfaces* **2013**, *5*, 3867−3874.
(40) Jin, L.; Yang, K.; Yao, K.; Zhang, S.; Tao, H.; Lee, S.-T.; Liu, Z.; Peng, R. Functionalized Graphene Oxide in Enzyme Engineering: A Selective Modulator for Enzyme Activity and Thermostability. *ACS Nano* **2012**, *6*, 4864−4875.
(41) De, M.; Chou, S. S.; Dravid, V. P. Graphene Oxide as an Enzyme Inhibitor: Modulation of Activity of α-Chymotrypsin. *J. Am. Chem. Soc.* **2011**, *133*, 17524−17527.
(42) Hummers, W. S., Jr; Offeman, R. E. Preparation of Graphitic Oxide. *J. Am. Chem. Soc.* **1958**, *80*, 1339−1339.
(43) Tan, X.; Feng, L.; Zhang, J.; Yang, K.; Zhang, S.; Liu, Z.; Peng, R. Functionalization of Graphene Oxide Generates a Unique Interface for Selective Serum Protein Interactions. *ACS Appl. Mater. Interfaces* **2013**, *5*, 1370−1377.
(44) Lowry, O. H.; Rosebrough, N. J.; Farr, A. L.; Randall, R. J. Protein Measurement with the Folin Phenol Reagent. *J. Biol. Chem.* **1951**, *193*, 265−275.
(45) Gonçalves, R.; Mateus, N.; De Freitas, V. Biological Relevance of the Interaction between Procyanidins and Trypsin: A Multitechnique Approach. *J. Agric. Food Chem.* **2010**, *58*, 11924−11931.
(46) Phillips, J. C.; Braun, R.; Wang, W.; Gumbart, J.; Tajkhorshid, E.; Villa, E.; Chipot, C.; Skeel, R. D.; Kale, L.; Schulten, K. Scalable Molecular Dynamics with NAMD. *J. Comput. Chem.* **2005**, *26*, 1781−1802.
(47) MacKerell, A. D.; Bashford, D.; Bellott; Dunbrack, R. L.; Evanseck, J. D.; Field, M. J.; Fischer, S.; Gao, J.; Guo, H.; Ha, S.; Joseph-McCarthy, D.; Kuchnir, L.; Kuczera, K.; Lau, F. T. K.; Mattos, C.; Michnick, S.; Ngo, T.; Nguyen, D. T.; Prodhom, B.; Reiher, W. E.; Roux, B.; Schlenkrich, M.; Smith, J. C.; Stote, R.; Straub, J.; Watanabe, M.; Wirkiewicz-Kuczera, J.; Yin, D.; Karplus, M. All-Atom Empirical Potential for Molecular Modeling and Dynamics Studies of Proteins. *J. Phys. Chem. B* **1998**, *102*, 3586−3616.
(48) Mayo, S. L.; Olafson, B. D.; Goddard, W. A. DREIDING: A Generic Force Field for Molecular Simulations. *J. Phys. Chem.* **1990**, *94*, 8897−8909.
(49) Banci, L.; Bertini, I.; Gray, H. B.; Luchinat, C.; Reddig, T.; Rosato, A.; Turano, P. Solution Structure of Oxidized Horse Heart Cytochrome c. *Biochemistry* **1997**, *36*, 9867−9877.
(50) Shih, C.-J.; Lin, S.; Sharma, R.; Strano, M. S.; Blankschtein, D. Understanding the pH-Dependent Behavior of Graphene Oxide Aqueous Solutions: A Comparative Experimental and Molecular Dynamics Simulation Study. *Langmuir* **2012**, *28*, 235−241.
(51) Medhekar, N. V.; Ramasubramaniam, A.; Ruoff, R. S.; Shenoy, V. B. Hydrogen Bond Networks in Graphene Oxide Composite Paper: Structure and Mechanical Properties. *ACS Nano* **2010**, *4*, 2300−2306.
(52) Argyris, D.; Tummala, N. R.; Striolo, A. Molecular Structure and Dynamics in Thin Water Films at the Silica and Graphite Surfaces. *J. Phys. Chem. C* **2008**, *112*, 13587−13599.
(53) Patra, N.; Wang, B.; Král, P. Nanodroplet Activated and Guided Folding of Graphene Nanostructures. *Nano Lett.* **2009**, *9*, 3766−3771.
(54) Jorgensen, W. L.; Chandrasekhar, J.; Madura, J. D.; Impey, R. W.; Klein, M. L. Comparison of Simple Potential Functions for Simulating Liquid Water. *J. Chem. Phys.* **1983**, *79*, 926−935.
(55) Park, S.; Khalili-Araghi, F.; Tajkhorshid, E.; Schulten, K. Free Energy Calculation from Steered Molecular Dynamics Simulations Using Jarzynski's Equality. *J. Chem. Phys.* **2003**, *119*, 3559−3566.
(56) Nosé, S. A Unified Formulation of the Constant Temperature Molecular Dynamics Methods. *J. Chem. Phys.* **1984**, *81*, 511−519.
(57) Blow, D. M.; Birktoft, J.; Hartley, B. S. Role of a Buried Acid Group in the Mechanism of Action of Chymotrypsin. *Nature* **1969**, *221*, 337−340.
(58) Sun, X.; Feng, Z.; Zhang, L.; Hou, T.; Li, Y. The Selective Interaction between Silica Nanoparticles and Enzymes from Molecular Dynamics Simulations. *PLoS One* **2014**, *9*, e107696.
(59) Vaitheeswaran, S.; Garcia, A. E. Protein Stability at a Carbon Nanotube Interface. *J. Chem. Phys.* **2011**, *134*, 125101.
(60) Calvaresi, M.; Hoefinger, S.; Zerbetto, F. Probing the Structure of Lysozyme−Carbon-Nanotube Hybrids with Molecular Dynamics. *Chem.—Eur. J.* **2012**, *18*, 4308−4313.

DOI: 10.1021/acsami.5b03118
ACS Appl. Mater. Interfaces 2015, 7, 12270−12277